*microorganisms*

MDPI

*Article*

# The Impact of Sea Ice Cover on Microbial Communities in Antarctic Shelf Sediments

**Marwa Baloza [1,2,*], Susann Henkel [1], Sabine Kasten [1,3,4], Moritz Holtappels [1,4,*] and Massimiliano Molari [5]**

[1] Alfred Wegener Institute Helmholtz Centre for Polar and Marine Research, Am Handelshafen 12, 27570 Bremerhaven, Germany; susann.henkel@awi.de (S.H.); sabine.kasten@awi.de (S.K.)
[2] Faculty 2 Biology/Chemistry, University of Bremen, Leobener Str., 28359 Bremen, Germany
[3] Faculty of Geosciences, University of Bremen, Klagenfurter Str., 28359 Bremen, Germany
[4] MARUM—Center for Marine Environmental Sciences, University of Bremen, 28359 Bremen, Germany
[5] HGF-MPG Joint Research Group for Deep-Sea Ecology and Technology, Max Planck Institute for Marine Microbiology, 28359 Bremen, Germany; mamolari@mpi-bremen.de
* Correspondence: marwa.baloza@awi.de (M.B.); moritz.holtappels@awi.de (M.H.)

**Abstract:** The area around the Antarctic Peninsula (AP) is facing rapid climatic and environmental changes, with so far unknown impacts on the benthic microbial communities of the continental shelves. In this study, we investigated the impact of contrasting sea ice cover on microbial community compositions in surface sediments from five stations along the eastern shelf of the AP using 16S ribosomal RNA (rRNA) gene sequencing. Redox conditions in sediments with long ice-free periods are characterized by a prevailing ferruginous zone, whereas a comparatively broad upper oxic zone is present at the heavily ice-covered station. Low ice cover stations were highly dominated by microbial communities of *Desulfobacterota* (mostly *Sva1033*, *Desulfobacteria*, and *Desulfobulbia*), *Myxococcota*, and *Sva0485*, whereas *Gammaproteobacteria*, *Alphaproteobacteria*, *Bacteroidota*, and *NB1-j* prevail at the heavy ice cover station. In the ferruginous zone, *Sva1033* was the dominant member of Desulfuromonadales for all stations and, along with eleven other taxa, showed significant positive correlations with dissolved Fe concentrations, suggesting a significant role in iron reduction or an ecological relationship with iron reducers. Our results indicate that sea ice cover and its effect on organic carbon fluxes are the major drivers for changes in benthic microbial communities, favoring potential iron reducers at stations with increased organic matter fluxes.

**Keywords:** benthic microbial communities; iron reducers; dissolved iron; pore-water profiles; redox zones; Sva1033



**Citation:** Baloza, M.; Henkel, S.; Kasten, S.; Holtappels, M.; Molari, M. The Impact of Sea Ice Cover on Microbial Communities in Antarctic Shelf Sediments. *Microorganisms* **2023**, *11*, 1572. https://doi.org/10.3390/microorganisms11061572

Academic Editor: Daolin Du

Received: 17 March 2023
Revised: 30 May 2023
Accepted: 3 June 2023
Published: 14 June 2023



## 1. Introduction

Shelf sediments play a significant role in the remineralization of organic matter (OM) and the recycling of nutrients and trace metals, e.g., [1–4]. In shelf regions, photosynthetic primary production accounts for 30–40% of organic matter supplied to the sea floor [5]. The majority of OM deposited at the seabed is remineralized while part of it is buried permanently, e.g., [6,7]. The remineralization of OM is mainly driven through microbially-mediated metabolic reactions using sequences of terminal electron accepting processes (TEAPs) with electron acceptors such as $O_2$ for aerobic respiration followed by $NO_3^-$, Mn(IV), Fe(III), $SO_4^{2-}$, and $CO_2$ for anaerobic respiration, e.g., [3,8–11]. The microbial remineralization of OM through the TEAPs is the main driver for biogeochemical processes in marine sediments [12–15] and is responsible for the formation of a typical/distinct sedimentary redox zonation, e.g., [8,11,16]. The extent of the different redox zones and the depth position of redox boundaries are mainly controlled by the reactivity and availability of terminal electron acceptors and OM accumulation rates, e.g., [8,16–18], suggesting that each of these zones is shaped by microbes with specific metabolic traits [19,20]. Therefore, differences in microbial community composition have been successfully used to decipher

the redox state and biogeochemical processes in a wide range of coastal marine and deep-sea sediments [21–28].

In the area of the Antarctic Peninsula (AP), the amount of organic matter originating from surface-water primary production is highly variable—both temporally and spatially—and depends mainly on the availability of light, which is regulated by season and sea ice cover [29–31]. During the spring-summer season, the melting of sea ice provides light for surface-water primary production with maximum production at the marginal ice zone [29]. On the other hand, the growth of sea ice cover during winter reduces light penetration, thereby limiting primary production. Sea ice cover thus controls the flux of OM to the seafloor. Baloza et al. [32] found that moderate sea ice cover (5–35%), which combines both favorable light conditions and water column stratification for algal growth, correlates with a high OM supply rate to the seabed. Previous studies have demonstrated that the quantity and quality of OM determine the microbial community composition, with certain taxonomic groups showing strong correlations with sedimentary parameters such as chlorophyll a concentration [23,33] and total organic carbon content [34–36].

Another factor regulating the production and subsequent deposition of OM over large parts of the Southern Ocean is the availability of dissolved iron (DFe), a limiting micronutrient for phytoplankton productivity, e.g., [37,38]. Iron supply can enhance phytoplankton growth resulting in higher sequestration of atmospheric $CO_2$ and enhanced accumulation of phytodetritus on the sea floor, a process known as the biological carbon pump [39,40]. Iron enters the Southern Ocean from various sources, with considerable variability in their estimated contribution. This includes iceberg-rafted debris (IRD) to sub-ice shelf, which contributes about 180–1400 Gg $a^{-1}$ of bioavailable Fe [41], followed by anoxic shelf sediments (7–790 Gg $a^{-1}$) [3], aeolian input (1.12 Gg $a^{-1}$) [41,42], and anoxic subglacial meltwaters (0.03–5.9 Gg $a^{-1}$) [43]. The importance of anoxic shelf sediments as a potential source of dissolved iron to the water column has recently been reported for Antarctic shelf sediments [3,32,44,45], and this source appears to be at least as significant as the input of iceberg–hosted material [3,44,46–48]. Therefore, identifying microbial key players involved in the iron cycle is essential, especially for the Southern Ocean, to better understand the factors that control iron bioavailability and efflux into the water column. At the moment, however, baseline knowledge about iron-reducing microbial taxa in Antarctic sediment is very limited [26,49].

In shelf sediments, dissimilatory microbial iron reduction (DIR) plays a key role in the remineralization of organic matter [3,26–28,32,45,50,51]. Predominantly, the microbial communities identified in performing DIR include bacterial taxa belonging to the order *Desulfuromonadales* (mostly those of the genera *Desulfuromonas*, *Desulfuromusa*, *Pelobacter*, *Geopsychrobacter*, and *Geothermobacter*) [52–57]. Furthermore, *Sva1033*, a clade of *Desulfuromonadales*, was identified by Ravenschlag et al. [58] and Wunder et al. [26] using RNA stable isotope probing experiments with permanently cold marine sediments from the Arctic and Sub-Antarctic, respectively. Both studies showed that the clade *Sva1033* has iron-reducing capabilities.

Sedimentary redox conditions along the eastern shelf of the AP have recently been investigated by Baloza et al. [32], who found that the supply of OM to the seafloor is mainly controlled by a sea ice cover. In areas of heavy ice cover, the low carbon supply coincides with low rates of benthic carbon remineralization. There, the surface sediments were characterized by a comparatively broad upper oxic zone of up to 4 cm with an underlying comparatively narrow ferruginous zone. With decreasing sea ice cover, an increase in carbon supply and benthic carbon remineralization rates was observed. At these sites, high dissolved iron concentrations of up to 400 µM were found at very shallow depths and below the ferruginous zones. A gradual decrease in sulfate concentrations and a steep increase in $H_2S$ concentrations marked the beginning of the sulfidic zone [32].

The present work on the microbial communities is complementary to the geochemical findings of Baloza et al. [32] and is based on the same set of sediment samples. The study is intended as a base study to evaluate the impact of changing sea ice conditions

on benthic microbial communities and—ultimately—nutrient fluxes across the sediment–water interface. We hypothesize that (i) the impacts of sea ice cover on organic matter fluxes are responsible for changes in benthic microbial communities, and (ii) the strong changes in redox zonation, induced by intense microbial organic matter remineralization rates, are coupled with an increment of iron-reducers at stations with increased organic matter fluxes. In order to test the two hypotheses, sediment samples from five stations along a 400 nautical mile transect with contrasting sea ice conditions were investigated by 16S ribosomal RNA (rRNA) gene sequencing. Correlation, multivariate regression, and differential taxa abundance analyses were performed to identify the main factors shaping the microbial community composition.

## 2. Materials and Methods

### *2.1. Sample Collection*

During research cruise PS118 with the German research vessel RV POLARSTERN (February–April 2019), sediments were collected from five stations along a 400-nautical mile transect from the eastern Antarctic Peninsula to the West of the South Orkney Islands (Figure 1; Table 1). In this study, we used sediments collected from five shelf stations at water depths ranging between 329 and 455 m to allow cross-comparison of sediment properties and OM turnover rates independent from water depth. The two deep stations (St5 and St6) were excluded from this study. At each station, a total of nine sediment cores with intact sediments and overlying water were collected from multiple deployments of a multi-corer (Oktopus GmbH, Kiel, Germany). Immediately upon retrieval, sediment cores were transferred to the ship's cool laboratory and placed in a water bath at 0 °C. Three cores were sliced on board to 0–1, 1–2, 2–3, 3–5, 5–7, and 14–16 cm layers and stored at −20 °C for DNA analysis. For pore-water and solid-phase analysis, six different cores were used and analyzed, as described previously by Baloza et al. [32].

**Table 1.** Description of investigated stations, including water depth, ice cover, moderate sea ice index, and bottom water temperature. The ice cover (30-year average of daily sea ice concentration) was calculated from historical satellite data of the Sea Ice Index, version 3 [59]. The moderate sea ice index is the relative occurrence of moderate ice cover (defined as 5–35% ice cover), weighted by the length of daylight (sunrise to sunset), as described by Baloza et al. [32]. Total organic carbon (TOC) from the upper five cm depth. The Total Carbon Remineralization Rate was calculated from diffusive fluxes of $O_2$, $NH_4^+$, DFe, DMn, and $S^{2-}$ using the equation from Baloza et al. [32]. The Total Carbon Supply Rate was calculated from the TOC removed in the upper layer due to aerobic C-remineralization added to the TOC accumulation rate.

| | Longitude | Latitude | Date | Water Depth | Ice Cover | Mod. Sea Ice Index | Bottom Water Temperature | TOC | Total Carbon Remineralization Rate | Total Carbon Supply Rate |
|---|---|---|---|---|---|---|---|---|---|---|
| | °W | °S | DD/MM/YYYY | m | % | | °C | wt% | mmol $m^{-2}$ $d^{-1}$ | mmol $m^{-2}$ $d^{-1}$ |
| Shelf St1 | 57.75 | 64.98 | 04/03/2019 | 428 | 81 | 0.038 | −1.9 | 0.71 | 1.134 | 2.67 |
| Shelf St2 | 55.90 | 63.97 | 11/03/2019 | 415 | 49 | 0.127 | −1.5 | 1.02 | 3.108 | 6.78 |
| Shelf St3 | 55.74 | 63.80 | 14/03/2019 | 455 | 47 | 0.084 | −1.2 | 0.19 | 1.452 | 3.20 |
| Shelf St4 | 54.33 | 63.05 | 17/03/2019 | 447 | 33 | 0.174 | −0.9 | 1.26 | 7.396 | 12.97 |
| Shelf St7 | 46.55 | 60.93 | 28/03/2019 | 329 | 28 | 0.092 | −0.1 | 0.60 | 1.833 | 2.50 |

### *2.2. DNA Extraction and Sequencing*

The DNA was extracted from 0.25 g of wet sediment using the DNeasy PowerSoil Kit (Q-BIOgene, Heidelberg, Germany) following the protocol provided by the manufacturer. Amplicon sequencing was conducted on an Illumina MiSeq machine at AWI laboratory. For the 16S rRNA gene amplicon library preparation, we used the bacterial primers 341F (5′-CCTACGGGNGGCWGCAG-3′) and 785R (50-GACTACHVGGGTATC TAATCC-30), which amplify the 16S rRNA gene hypervariable region V3–V4 in Bacteria (400–425 bp fragment length). The amplicon library was sequenced with MiSeq v3 chemistry in a 2 × 300 bp paired-end run with >50,000 reads per library, following the standard instructions of the

16S Metagenomic Sequencing Library Preparation protocol (Illumina, Inc., San Diego, CA, USA).

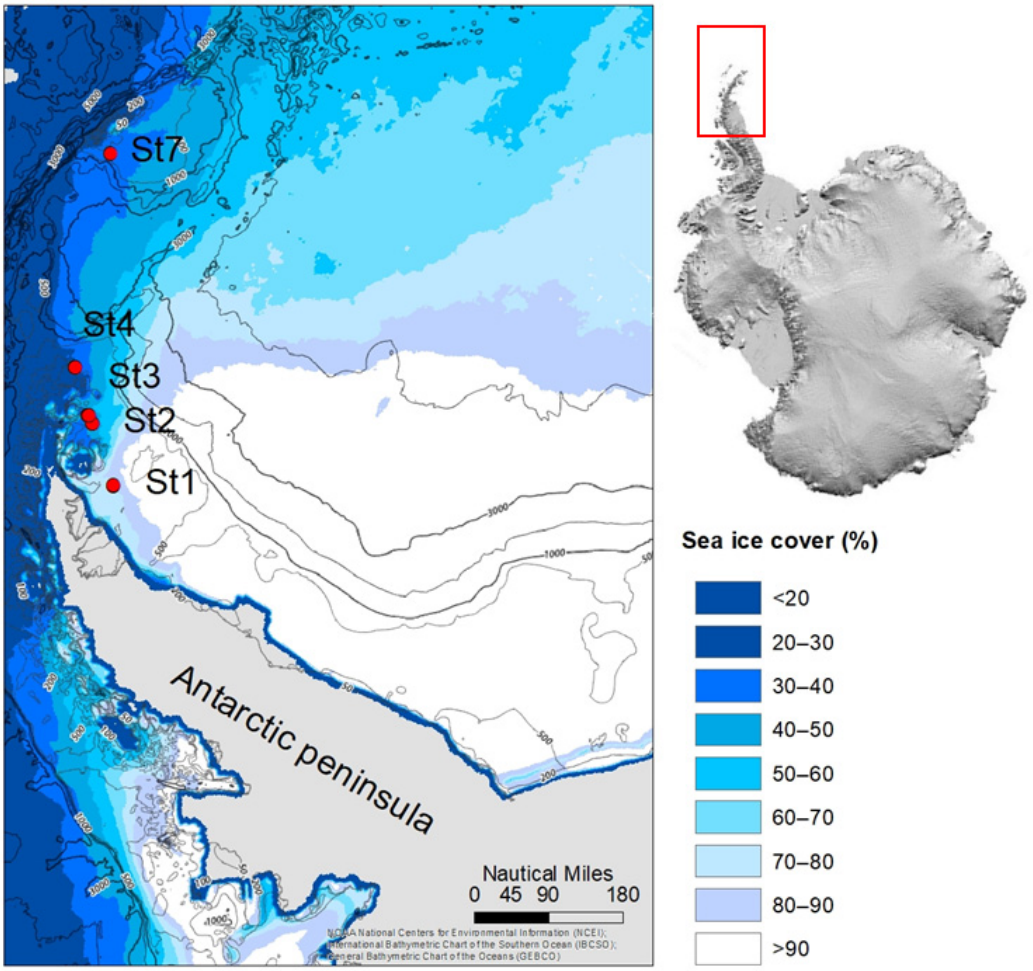


**Figure 1.** Map showing the Antarctic Peninsula with the locations of the sampled stations (red circles with station numbers) during the PS118 expedition modified after Baloza et al. [32]. Colors denote the proportion of time the ocean is covered by sea ice of concentration 85% or higher as calculated from AMSR-E satellite estimates of daily sea ice cover at 3.37 nautical mile resolution [60]. Water depth is indicated by isolines.

### *2.3. Amplicon Data Analysis*

The quality cleaning of the sequences was performed using several software tools. The first tool was Cutadapt [61], which was used to remove the attached primers from the data. Then, DADA2 packages in R [62] were used for filtering and trimming low-quality sequences. Further, sequences with more than two expected errors were removed depending on their quality profiles. DADA2 was also used to merge the filtered forward and reverse reads and remove Chimeras from the denoised output. For the taxonomic classification, the SILVA 138 database [63] was used, and sequences with less than 90% of similarity with SILVA sequences were removed from the dataset. Absolute singletons (i.e., which refer to ASV sequence occurring only once in the full dataset) [64], contaminant sequences (as observed in the negative control), and unspecific sequences (i.e., unclassified sequences at the domain level, chloroplast, and mitochondrial sequences) were removed from amplicon datasets before the statistical analysis. The total number of reads per sample was summarized in an amplicon sequence variants (ASVs) table (Table S1).

All statistical analyses were conducted using RStudio v4.0.2; R Core [65]. Sample data matrices and alpha diversity indices were generated using the R package 'phyloseq'

v1.32.0 [66]. The rarefaction curves for each sample were generated based on 50 equally spaced rarefied sample sizes with 100 iterations. Non-metric multidimensional scaling (NMDS) analysis was conducted on Euclidean distance matrix based on ASV abundances that have undergone centered log-ratio (CLR) transformation using R package 'vegan' v2.5.7 [67] and 'Composition' v2.0.4 [68], respectively. Differences in bacterial communities between groups of stations, defined based on sea ice cover, were tested with analysis of similarities (ANOSIM) in the R package 'vegan' v2.5.7 [67]. Furthermore, the significance of the relationship between the frequency of moderate sea ice conditions, sediment depth, and community composition was tested using permanova tests (9999 unrestricted permutations; $p$-values < 0.05) with 'vegan' v2.5.7 [67]. Geochemical parameters that shape microbial community compositions were standardized (z-scoring) and tested for predictor variable collinearity, then investigated to determine the correlations between geochemical parameters and bacterial community compositions by distance-based redundancy analysis (dbRDA) in the R package 'vegan' v2.5.7 [67]. The significance of the relationship between explanatory variables and community composition was tested using Monte Carlo permutation tests (9999 unrestricted permutations; with $p$-value < 0.05).

In order to identify taxonomical associations with iron cycling of all shelf stations, the Metastats-test-based differential abundance analysis of taxa was performed using the ALDEx2 package v1.20.0 [69] at a significance threshold of <0.01 for the parametric test (glm.eBH) and non-parametric test (kw.ep). This analysis was done to examine the different bacterial taxa between the upper 3 cm of sediment of Shelf St4 dominated by ferruginous conditions against the upper 3 cm of Shelf St1 in which oxic respiration is the dominant process for OM degradation. Linear regression between centered log-ratio values of the ASV highly abundant in the ferruginous zone and dissolved iron (DFe) concentrations (in µmol/L) for the five shelf stations was performed using Pearson's correlations at $p < 0.05$. Furthermore, the environment coverage for the most closely related sequences (>99% similarity) to ASV highly abundant in the ferruginous zone was identified with BLASTn (GeneBank nucleotide database, 11 March 2022) and reported for each ASV.

## 3. Results

### *3.1. Bacterial Diversity and Sequencing Data Normalization*

Using Illumina 16S rRNA amplicon sequencing of the V3–V4 hypervariable region, we obtained a final dataset of 4,252,065 reads (amplicons) in 90 samples, which were assigned to 38,655 ASVs belonging to bacterial taxonomies of 64 phyla, 162 classes, 378 orders, 536 families, and 786 genera. Rarefaction profiles of 16S rRNA gene sequences reached a plateau for most of the samples (Figure S1). Sediments hosted from hundreds to thousands of ASVs in each station were investigated. The highest bacterial richness (measured as the number of ASVs per sample) was observed in the uppermost sediments from all stations. However, bacterial diversity (measured with the observed richness, Shannon index and the inverse Simpson index) decreased northward in the AP surface sediments and differed among sediment depths (Table S1, Figure S1). Overall, the heavy ice-covered station (St1) had the highest species richness and diversity of all stations.

Sample read counts ranged from 942 to 250,824 per sample (Table S1), the median sequencing depth was 30,167, and the 75th percentile and the 25th percentile were 55,749 and 18,651, respectively (Table S1). To check whether the uneven sequencing depth could introduce bias in the analysis of microbial communities between stations/layers, we tested if there is a significant correlation between the original dataset and the dataset that is normalized by a fixed number of reads. We normalized the dataset to the median sequencing depth (30,000) and to the smallest number of reads (942). Our results showed high correlations between the original dataset and the dataset that is normalized to the median sequencing depth (Mantel statistic r: 0.99, Significance: $1 \times 10^{-4}$). In contrast, the original dataset and the normalized dataset to the smallest number of reads did not significantly correlate (Mantel statistic r = 0.047, Significance: 0.2035). Based on this result, the original dataset was used for further analysis.

### *3.2. Effect of Sea Ice Cover and Geochemistry on Bacterial Community Structure*

Non-metric multidimensional scaling of ASVs did not show any clear pattern between stations (Figure 2A). However, when similarity in bacterial community structure was investigated between the stations grouped according to sea ice cover, the ANOSIM showed that bacterial communities between heavy ice cover and low ice cover stations are significantly different (ANOSIM, $r > 0.53$, $p < 0.001$). This result suggests that sea ice cover is a variable affecting the microbial community composition in the AP shelf sediments. To further test the contribution of sea ice cover in explaining differences in the microbial community, a permanova test was carried out, also including sediment depth as an explanatory factor, which is an important environmental constraint for microbes (Table S2). The permanova test showed that the frequency of moderate sea ice conditions (here defined as 5–35% sea ice cover) is significantly different between stations ($p < 0.0001$) and can explain 4% (when testing all sediment depths) to 13% (when testing the surface layers only) of the variation between microbial communities. Sediment depth was also tested as another factor affecting the microbial community structure. The results showed a significant difference between sediment depths ($p < 0.0001$), explaining 9% of the variance.

In order to identify the potential geochemical parameters that correlate with the microbial communities across all sites, a dbRDA was performed (Figure 2B, $F = 2.90$, $p < 0.001$, Df: 7, 81). The factors of $O_2$, DFe, DIC, $SO_4^{2-}$, Fe(III)/Al, S/Al, and the C/N ratio were included as explanatory variables in the model and together explained 20% of the total variation in the bacterial community. The variance inflation factor between these variables was below five (VIF = 4.3), indicating independence between variables. The total organic carbon content (TOC) was not used as an explanatory variable due to collinearity to other variables such as DIC, $SO_4^{2-}$, Fe (III)/Al and S/Al. $NH_4^+$. $H_2S$ was also removed from this data analysis as it correlated with DIC and $SO_4^{2-}$, respectively. However, we used the sulfur content in the solid phase (S/Al) instead of $H_2S$ as an indication of sulfate reduction and accumulation of pyrite.

Community composition between high ice cover and low ice cover stations was described mainly by the increase of $O_2$ ($F = 3.754$, $p = 0.003$) and DFe concentrations ($F = 3.703$, $p = 0.003$), followed by S/Al ($F = 2.190$, $p = 0.005$), Fe/Al ($F = 2.009$, $p = 0.005$), then C/N ratio ($F = 1.868$, $p = 0.011$), DIC ($F = 1.636$, $p = 0.025$), and $SO_4^{2-}$ ($F = 0.954$, $p = 0.476$). In accordance with the NMDS ordination (Figure 2A,B), oxic layers at the heavy ice cover station exhibited a strong separation of bacterial communities from the low ice cover stations. However, anoxic layers at the heavy ice cover station tend to cluster together with the low ice cover stations. The model strongly attributed this distinction to $O_2$ and DFe differences between groups.

### *3.3. Patterns in Bacterial Community Composition*

Figure 3 shows the relative abundance of the 30 most abundant taxa (> 0.1%) across all five shelf stations. Across all stations, similarities in the distribution of benthic microbial communities have been observed. Dominant taxa belonged mostly to Gammaproteobacteria and Woeseia, Bacteroidota (mostly Bacteroidia), and NB1-j were present in all sediment depths and represented >15% of the total microbial community (Figure 3). Distinct differences in the benthic microbial communities between heavy ice cover (Shelf St1) and low ice cover stations (Shelf St2, St3, St4 and St7) were also evident. Surface sediments of the low ice cover stations were dominated by anaerobic bacterial groups belonging to Proteobacteria (i.e., Halioglobus, order_B2M28, OM60(NOR5) clade, family_Rhodobacteraceae, and order_BD7-8) (>13%), Desulfobacterota (i.e., order_Sva1033, family_Desulfocapsaceae, order_Desulfobulbales, phylum_Desulfobacterota, family_Desulfosarcinaceae, Sva0081 sediment group) (>16%) Sva0485 (3%), and Bacteroidota (i.e., Lutibacter, Lutimonas, family_Bacteroidetes BD2-2, class_Bacteroidia, family_Flavobacteriaceae) (10%) within the upper 3 cm of sediment. However, unlike the low ice cover stations, abundances of Desulfobacterota (order_Desulfobulbales, phylum_Desulfobacterota, family_Desulfosarcinaceae, Sva0081 sediment group) Sva0485, and Bacteroidota (i.e., Lutibacter, Lutimonas, fam-

ily_Bacteroidetes BD2-2) were very low (<0.1%) in the top 3 cm of the heavy ice cover station (Shelf St1) where oxic respiration dominated OM degradation. At the same site, the relative abundance of Proteobacteria (i.e., order_BD7-8, class_Alphaproteobacteria, order_AT-s2-59) (>5%), Desulfobacterota (i.e., order_Sva1033, family_Desulfocapsaceae, phylum_Desulfobacterota) (>7%), Sva0485 (1.4%) and Bacteroidota (i.e., Lutibacter, Lutimonas, family_Bacteroidetes BD2-2, class_Bacteroidia) (8.5%) increased with depth (in the ferruginous zone). Importantly, Sva1033, a clade of Desulfuromonadia, was highly abundant within the top 3 cm of the sediment at the low ice cover stations (>7%) and at the sulfate reduction zones at 14 cm depth (>4%). Except for the high ice cover station, the highest abundance of Sva1033 occurred below 3 cm sediment at the ferruginous zone (>4%). In addition, sequences related to known sulfate reducers, such as Desulfobacterota (mostly Desulfobacteria and Desulfobulbia), Myxococcota (mostly Polyangia), and Sva0485 were highly abundant at 14 cm layer at low ice cover stations (14%) compare to the heavy ice cover station (<3%; at 14 cm layer).

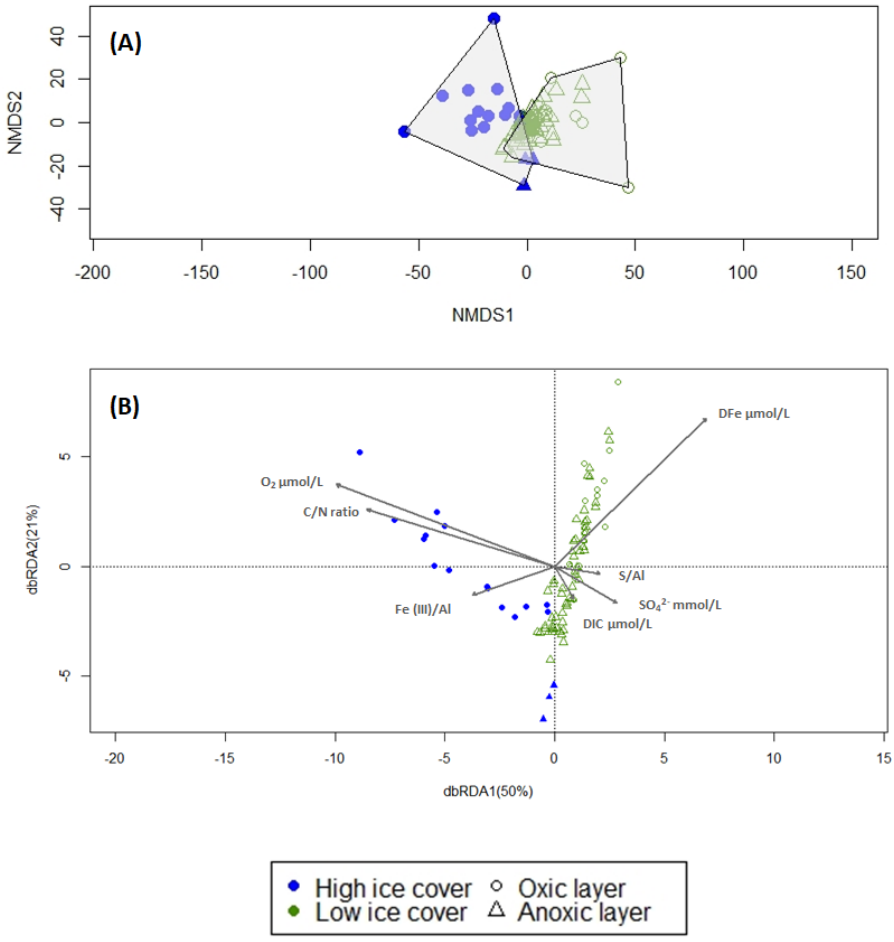


**Figure 2.** Microbial community composition of all five shelf stations. (**A**) Non-metric Multidimensional Scaling (NMDS) ordination of microbial community composition based on Euclidean distance after transforming the data using CLR for stations under high ice cover (Shelf St1) and low ice cover (Shelf St2, St3, St4, St7) (stress value = 0.152, $R^2$ = 0.98). (**B**) Distance-based redundancy analysis (dbRDA) ordination plot of bacterial communities. Sample points in panels A and B are distinguished by site and sediment depth (oxic and anoxic layer) and by color and shape, respectively. dbRDA1 (variation 50%) and dbRDA2 (variation 21%) axes are displayed, which constrain the Euclidean distance matrix with geochemical parameters $O_2$, DFe, DIC, $SO_4^{2-}$, Fe(III)/Al, S/Al, C/N ratio. The total model (F = 2.90, $p < 0.001$, Df: 7, 81) and each individual parameter ($p < 0.05$) were significant except for $SO_4^{2-}$.

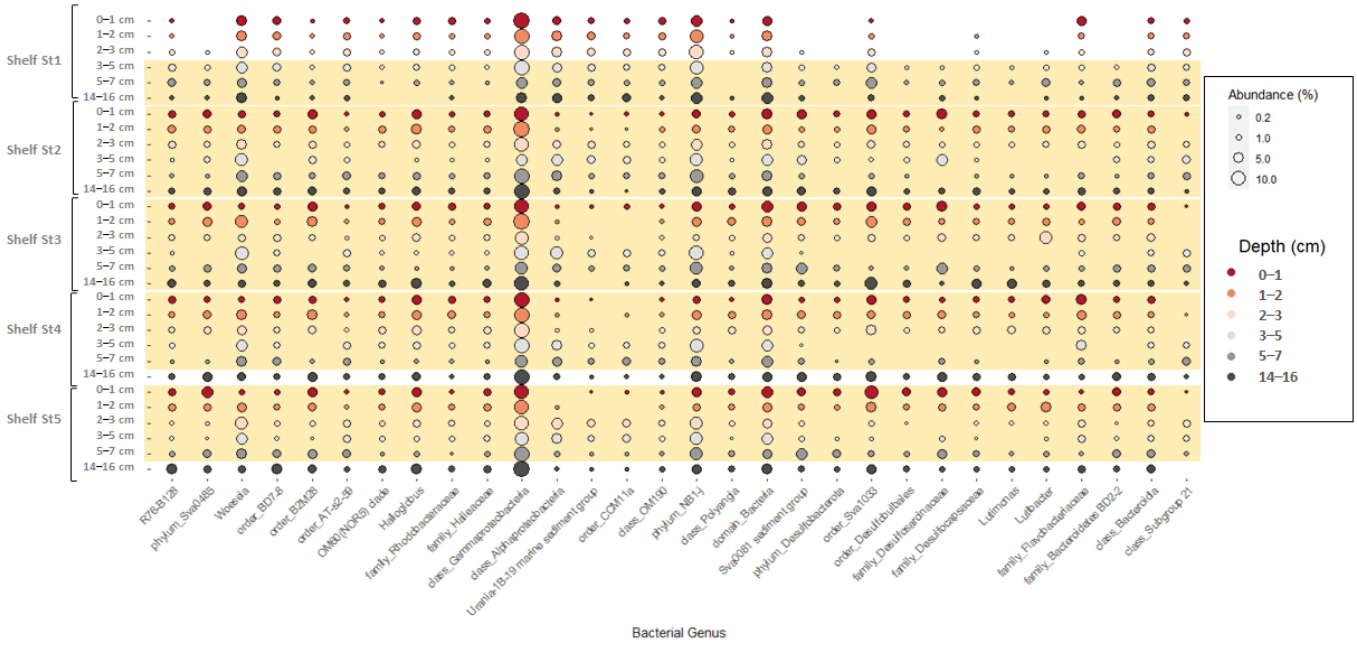


**Figure 3.** Microbial community composition in five shelf stations across the eastern coast of the Antarctic Peninsula. The relative abundance of bacterial 16S rRNA genes (cut-off > 0.1%) at genus-level resolution is shown for six sediment layers. For those taxa unclassified at genus, the higher taxonomic level is reported. Orange shadings represent the ferruginous zone in each station.

### *3.4. Potential Iron-Reducing Bacteria*

The results of the differential abundance analysis between the ferruginous zone at Shelf St4 against the oxic zone at Shelf St1 revealed that 791 ASVs were significantly different between the two stations (Shelf St1 + Shelf St4) ($p < 0.05$; Table S3). Among these taxa, 12 ASVs contributed individually to more than 1% of the total community at the ferruginous zone, contributing together up to 14–20% at low ice cover stations in contrast to only <6% at the high ice cover station of bacteria community in the ferruginous zone. The major groups of bacteria present were identified as members of Sva1033 (class Desulfuromonadia), SEEP-SRB4 (class Desulfobulbia), Persicirhabdus (class Verrucomicrobiae), Halioglobus, order_B2M28 and OM60 (NOR5) clade (class Gammaproteobacteria), Maribacter and Lutimonas (class Bacteroidia) and class Polyangia.

Across all stations, the relative abundance of 12 putative Fe-reducing bacterial taxa show similar patterns along sediment profiles mirroring dissolved iron profiles (Figure 4). Sva1033 was the most abundant taxon in the ferruginous sediments, with a peak in the relative abundance at the same depth as the highest dissolved Fe concentrations (Figure 4). The relative abundance of Sva1033 was highest (>5%) near the sediment surface at low ice cover stations (Shelf St2, St3, St4, and St7) compared to the high ice cover station where the iron reduction zone is deeper (below 4 cm depth). There, its relative abundance was <2% at the surface and 0.3% below 5 cm depth (Figure 4).

Furthermore, significant positive correlations between centered log-ratio values of putative Fe-reducing bacteria and dissolved Fe concentrations were observed for all potential iron-reducers ($p < 0.05$), except for order_B2M28, where $p = 0.08$ (Figure 5). The class_Gammaproteobacteria (asv4) showed the highest correlation with DFe concentrations, followed by Lutimonas (asv26), while order_B2M28 (asv6) had the weakest correlation (Figure 5).

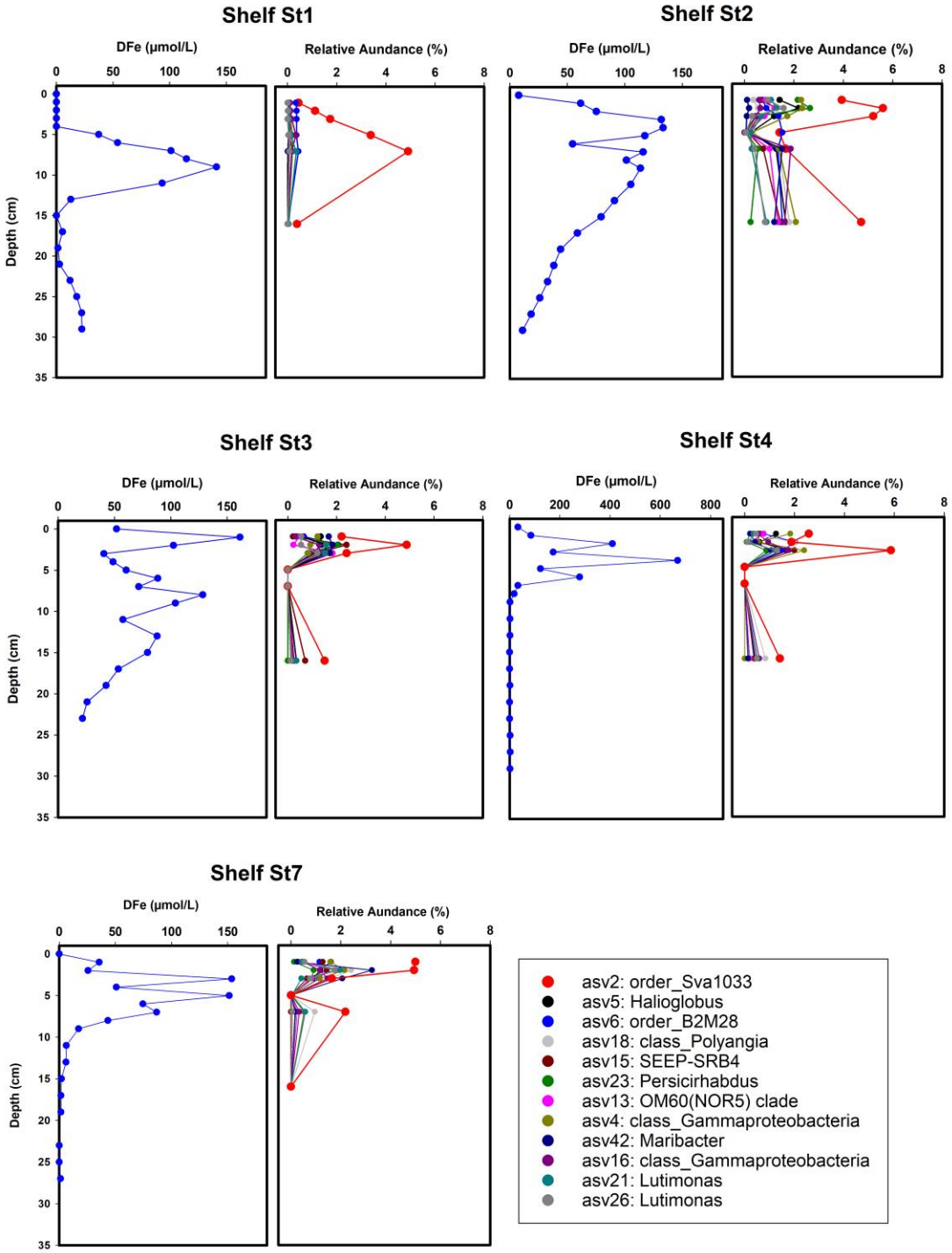


**Figure 4.** Representative profiles of the depth distribution of abundances of putative Fe-reducing bacteria in relation to dissolved iron (DFe) concentrations. Twelve different taxa were identified by applying differential abundance analysis. The relative abundance for each taxon was estimated from one sediment core. DFe concentrations were measured in a core near (<1 m) the collected microbial samples.

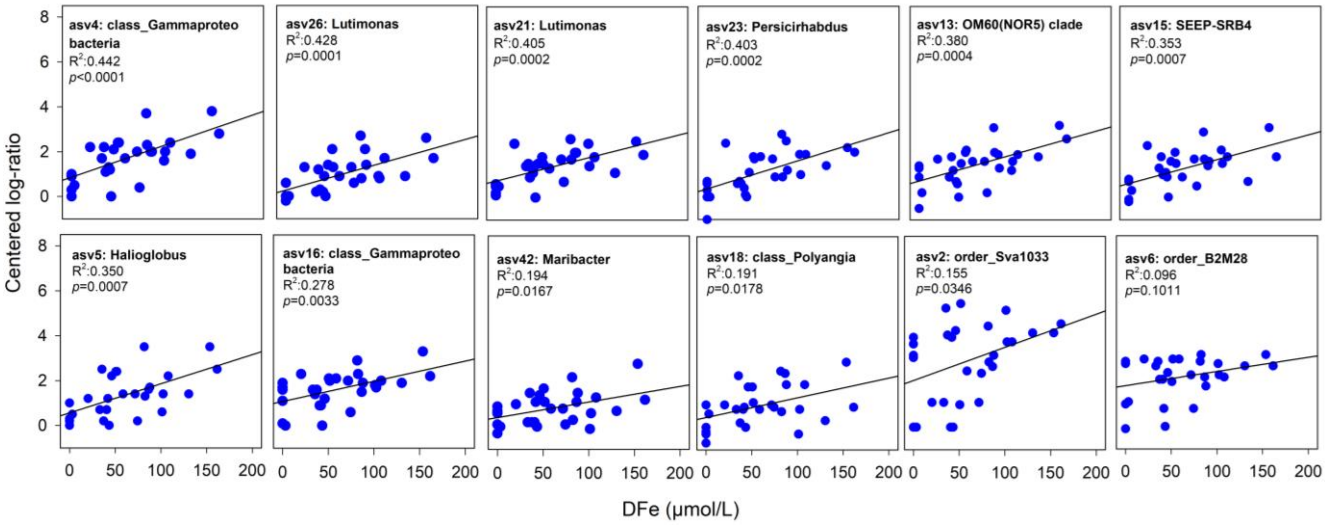


**Figure 5.** Linear regression between centered log-ratio values of putative Fe-reducing bacteria and DFe concentrations (in µmol/L) for five shelf stations. Linear models' $R^2$, Pearson's correlations, and their *p*-value are reported in each panel. The centered log ratio of putative Fe-reducing bacteria used in the correlations is the average of two sediment cores. At Shelf St4, only five depths were used in the correlations. The last depth was excluded as it is below the ferruginous zone.

For the 12 putative Fe-reducing bacterial taxa, sequence homology searches within GenBank with the highest similarity (e.g., 100% or >99%) were performed using BLASTn (NCBI website) (Table S4). The most closely related sequences were retrieved from the permanently cold marine sediment (e.g., Arctic and Antarctic; 31%) [58,70–76], from suboxic sediment (23%) [52,77], from methane seep sediment (17%) [77–81], from tidal flat sediment (17%), and from hydrothermal or mud volcanos sediments and deposits (9%) (Figure 6 and Table S4).

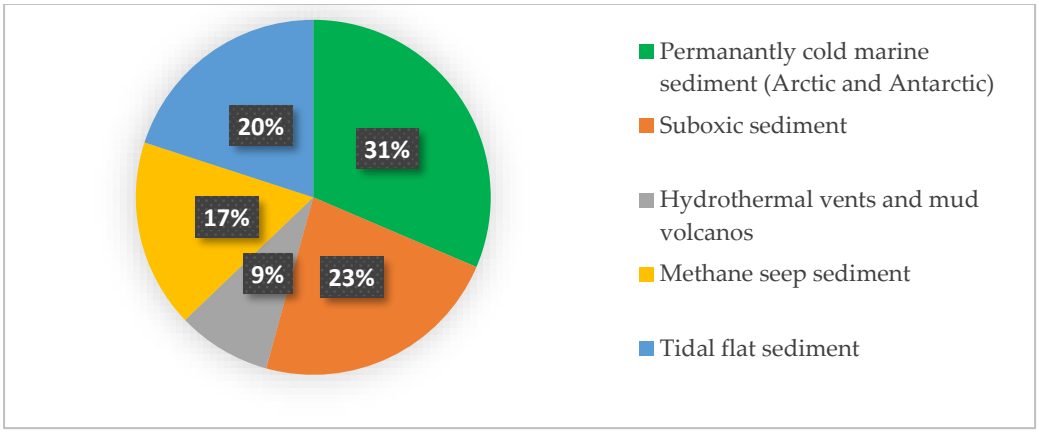


**Figure 6.** Environmental distribution for the most closely related sequences (>99% similarity) to ASV highly abundant in the ferruginous zone. For details, see Table S2.

## 4. Discussion

The Antarctic Peninsula is projected to undergo profound climatic and environmental changes affecting seasonal sea ice cover, water column stratification, terrestrial meltwater run-off, and related nutrient input, and thus the conditions for primary production, organic carbon (OC) export, and benthic remineralization [32,82,83]. The impact of sea ice cover on microbial communities in underlying sediments is currently understudied. We hypothesize that (i) the impact of sea ice cover on organic matter fluxes are responsible for changes in benthic microbial communities, (ii) the strong changes in redox zonation, induced by

intense microbial organic matter remineralization rates, are coupled with an increment of iron-reducers at stations with increased organic matter fluxes. In order to test the two hypotheses, microbial community composition at different sites with contrasting sea ice conditions along the eastern shelf of the AP was analyzed using 16S ribosomal RNA (rRNA) gene sequencing in surface (top 16 cm) sediments. Our findings, as discussed below, confirmed our hypotheses, showing that the effect of sea ice cover on organic carbon fluxes is the major driver for the variability in benthic microbial communities and redox zonation in the sediments of the eastern coast of the AP. Importantly, at low ice cover stations, characterized by high carbon supply and remineralization rates, we identified the dominance of potential iron-reducing bacteria (up to 20% of total sequences; Figure 4).

In this study, we observed that benthic microbial communities are significantly different between sites with high and low ice cover. Recently, a biogeochemical study of sediments from the exact same stations [32] described sea ice conditions as the main factor controlling rates of organic carbon supply and benthic remineralization. A low carbon supply rate of 2.7 mmol C $m^{-2}$ $d^{-1}$ was measured for the station with heavy ice cover, explained by limited light availability and thus low surface-water primary production. In contrast, the locations with low sea ice cover showed high carbon supply rates of up to 13.0 mmol C $m^{-2}$ $d^{-1}$, indicating that primary and export production are both enhanced when both light and water column stratification is sufficient to support phytoplankton growth. This scenario is supported by known large phytoplankton blooms and high primary production during spring/summer seasons on the marginal ice zone along the AP [84–87]. Our results are in agreement with the previous studies on bacterial communities in marine Antarctic surface sediments [33,34]. Currier et al. [33] also found that the structure and composition of benthic microbial communities reflect the condition of sea ice cover. Microbial communities underlying first-year sea ice cover are highly dominated by heterotrophic algal polysaccharide degrading taxa and sulfate-reducing bacteria and correlate with higher chlorophyll a and total organic carbon content, reflecting increased surface-water productivity and high OC fluxes to the seafloor [33]. Conversely, in sediments underlying multi-year sea ice cover, an enrichment of known archaeal and bacterial chemoautotrophs was found with considerably lower chlorophyll a and TOC contents, reflecting low surface-water primary production [33]. In addition, Learman et al. [34] found that the variability in the benthic microbial community composition along the Antarctic surface sediment is mainly driven by the quality and quantity of organic matter and the availability of nutrients. These findings agree with the results of our study that the impact of sea ice cover on organic matter fluxes is the main factor structuring the benthic microbial communities along the AP in such a way that they select the microorganisms that best respond to the given conditions.

The gradual decrease in sea ice cover along the transect of the investigated sites, accompanied by an increase in organic C-supply rates, have resulted in a distinctly different redox zonation of the underlying sediments suggesting that the different redox conditions are shaped by organic C burial rates and the activity of microorganisms with specific metabolic traits. Sediments at the heavy ice cover station were characterized by a low carbon remineralization rate of 1.1 mmol $m^{-2}$ $d^{-1}$ and a deeper oxygen penetration depth compared to stations with low ice cover (6.3 $\pm$ 0.7 cm and 1.8 $\pm$ 0.02 to 0.5 $\pm$ 0.07 cm, respectively) (Figure S2), resulting in the upper boundary of the ferruginous zone to be located below 5 cm depth [32]. However, unlike the heavy ice cover station, sediments of the low ice cover stations showed high benthic carbon remineralization rates (1.8–7.3 mmol $m^{-2}$ $d^{-1}$), resulting in a more condensed redox zonation and high concentrations of dissolved Fe (>400 µM at Shelf St4) close to the sediment surface (Figure S2). Below the ferruginous zone, the gradual increase of $H_2S$ concentrations below 10 cm depth was detected, marking the beginning of the sulfate reduction zone (Figure S2). In accordance with these observations, we found that the differences in microbial community composition between the high ice cover and the low ice cover stations are largely explained by dissolved $O_2$ and Fe concentrations in pore water (Figure 2B), which are fundamentally different in the uppermost sediment

between stations with high and low ice cover (Figure 2B). This indicates that microbial communities in the surface sediments of the high ice cover station are mainly dominated by aerobes. In contrast, the variation in community composition over sediment depth at the stations with low ice cover was explained mainly by the variability of dissolved Fe concentration, S/Al, DIC, and $SO_4^{2-}$ (Figure 2B), suggesting that iron and sulfate-reducing bacteria are the dominant players.

Microbial communities in surface sediments (i.e., 0–1 cm) of all stations are dominated by bacterial groups belonging to *Gammaproteobacteria*, *Alphaproteobacteria*, *Bacteroidota*, and *NB1-j*, which were often detected during the initial degradation of algal-derived organic matter [22,75,88,89]. At the low ice cover stations, anaerobic bacterial communities of iron and sulfate reducers (31% at Shelf St4 to 41% at Shelf St7) were more abundant at these sites compared to the heavy ice cover station. The relative abundance of *Desulfobacterota* (mostly order_Sva1033, family_*Desulfocapsaceae*, phylum_*Desulfobacterota*), which harbor many species of iron reducer taxa [25,26,54,90] and sequences related to known sulfate reducers, such as *Desulfobacterota* (mostly *Desulfobacteria* and *Desulfobulbia*), *Myxococcota* (mostly *Polyangia*), and *Sva0485* were abundant near the sediment surface of low ice cover (>20%) and at greater depth (14 cm depth) (>12%). Similarly, some of those taxa have been previously observed in shallower depths in more reducing shelf sediments of the Sub-Antarctic island of South Georgia [26] and Arctic fjords [91]. Unlike the low ice cover stations, the relative abundance of anaerobic microbial communities of Desulfobacterota at the heavy ice cover station increased below the oxic zone and reached the highest relative abundance (>10%) within the ferruginous zone, reflecting low burial rates of organic matter.

Furthermore, the high relative abundance of sulfate reducers in the ferruginous zone at the sites with low ice cover can be explained by the tight link between the biogeochemical cycles of iron and sulfur. For this reason, Fe liberation into the pore water can result either from dissimilatory iron reduction (DIR) or happen abiotically related to sulfide oxidation by Fe(III) reduction, e.g., [92]. The tight coupling of the post-depositional iron and sulfur cycles has been demonstrated recently based on geochemical data from the Argentina continental margin [93], Arctic sediments [94,95] and (sub-)Antarctic sediments [26]. Wunder et al. [26] suggested that the high relative abundance of sulfate reducers in the ferruginous zones is due to sulfate reduction masked by the reoxidation of the produced sulfide to sulfate via Fe(III) reduction supporting the persistence of sulfate reducers.

The anoxic shelf sediments have recently been considered a potential source of bioavailable Fe to Antarctic coastal waters and beyond [3]. Along the sampling transect of the AP, elevated upward fluxes of DFe in the sediment were detected at the low ice cover stations (52 to 171 μmol $m^{-2}$ $d^{-1}$), while a low upward flux of DFe was observed at the heavy ice cover station (17.7 μmol $m^{-2}$ $d^{-1}$). The steep concentration gradients of DFe close to the sediment surface indicate that more DFe might escape from shelf sediments into the water column highlighting the importance of sediments underlying low ice cover as a potential source for limiting nutrients to the shelf waters [32]. To identify taxa potentially involved in the sedimentary biogeochemical cycling of iron, we investigated differences in bacterial community composition under different DFe fluxes.

At all sites, the distribution of *Sva1033*, a clade of Desulfuromonadia, is tightly coupled to the increase in the dissolved iron concentration showing the steepest slope in the linear regression (Figure 5). At low ice cover stations, Sva1033 increased close to surface sediment and peaked in abundance (>7%) at several centimeter depths where iron reduction predominates. Only sediments at the heavy ice cover station where the ferruginous zone is located at greater sediment depth, the relative abundance of *Sva1033* decreased (<2%) near to sediment surface while it increased (>4%) below 5 cm depth in the ferruginous zone (Figure 4). Members of this clade were detected previously in the ferruginous sediments of the (sub-) Antarctic [26] and Arctic shelf [25,58] and were suggested to be responsible for the iron reduction in these permanently cold marine sediments. Their metabolic capabilities to reduce iron have been confirmed recently by incubation experiments of Antarctic

Potter Cove sediments using RNA stable isotope probing [26]. Our results provide further evidence that *Sva1033* plays an active role in the cycling of iron in Antarctic sediments.

Other putatively Fe-reducing bacterial taxa identified in this study besides Sva1033 (class *Desulfuromonadia*) are *SEEP-SRB4* (class *Desulfobulbia*), *Persicirhabdus* (class *Verrucomicrobiae*), *Halioglobus*, *order_B2M28* and *OM60 (NOR5)* clade (class *Gammaproteobacteria*), *Maribacter* and *Lutimonas* (class *Bacteroidia*) and class *Polyangia* (Figures 4 and 5). Members of these groups make up the bulk of sedimentary anaerobic communities in the ferruginous zones, and some of them were shown previously to be present in marine sediments with high dissolved iron and manganese concentrations [52,70–72,80,96], suggesting an important role in meditating metal biogeochemical cycling. Moreover, the results of the environmental distribution for the most closely related sequences (>99% similarity) reveal that >70% of these taxa were detected before in permanently cold marine sediments (e.g., Antarctic and Arctic) [22,26,58,70–74] and various deep-sea environments [77–80,96], indicating that most of these taxa are psychrophilic (Figure 6).

An increase in the relative sequence abundance of putatively Fe-reducing bacterial taxa in the ferruginous zone at both high ice cover and low ice cover stations (Figures 4 and 5) provides evidence that they might be involved in DIR in surface sediments of the AP or have syntrophic partnerships and/or common metabolic preferences with iron reducers. Future work should explore the in situ metabolic activity of these potential Fe-reducing bacterial taxa, with a particular focus on Sva1033, to better understand factors that control iron bioavailability and potential efflux into the water column from Antarctic and Southern Ocean shelf sediments.

The extent of Antarctic sea ice has undergone a drastic decline since 2015, indicating increased interannual variability [83]. Model projections further indicate a continued decline in the near future [97]. Our results show that the melting of sea ice sustains favorable light conditions and water column stratification, resulting in increased primary productivity and organic matter flux to the seafloor [32]. These changes, in turn, have an impact on the activity and composition of benthic microbial communities. Consequently, the regional (southward) shift in sea ice cover could potentially lead to an increase in benthic remineralization rates, promoting a shift in microbial communities towards anaerobic taxa and an increase in benthic iron fluxes. The latter could have positive feedback on primary production in the water column, further stimulating the overall process.

## 5. Conclusions

Our study reveals that sea ice cover and associated carbon burial fluxes explain up to 13% of the variability between microbial communities in the AP shelf sediments. At all stations, *Sva1033* was the dominant member of Desulfuromonadales in the ferruginous sediments, which confirms its putative role in reducing iron oxide minerals in permanently cold marine sediments. Furthermore, our approach identified for the first time other taxa that might contribute to the benthic iron cycle or have ecological relationships with the dominant iron reducers. The significant contribution of potential iron reducers (up to 15%) to microbial communities reveals the importance of sediments underlying low ice cover as a potential source of dissolved iron to shelf waters. In this regard, the findings reported here expand our knowledge about changes induced by the increase of OM load to microbial community composition in AP shelf sediments under contracting sea ice cover and stimulate future research to better elucidate the role of microbial iron reducers in the biogeochemical iron cycle.

**Supplementary Materials:** The following supporting information can be downloaded at: https://www.mdpi.com/article/10.3390/microorganisms11061572/s1, Table S1: Overview of sampled stations during RV Polarstern expedition PS118. The table consists of sampling information for each station, number of sequences in each step of the bioinformatics workflow as well as alpha diversity indices: (1) observed richness, (2) Shannon and (3) inverse Simpson, conducted using the R package 'phyloseq'. Table S2: Output PERMANOVA and distance-based redundancy analysis (dbRDA). Table S3: ASVs highly abundant in the ferruginous zone. Differential abundance of taxa

between surface sediments (0–3 cm) of stations Shelf St1 and Shelf St4 samples according to the *t*-test based metastats analysis. Differentially abundant taxa having statistically significant differences for parametric test (glm.eBH) ($p < 0.01$) and non-parametric test (kw.ep) ($p < 0.05$) are reported for each ASV per sample. Table S4: The most closely related sequences with identity (ID) >99%, as identified with BLASTn (GeneBank nucleotide database, 12 June 2022). Figure S1: Diversity indices for bacterial communities in six different depths for five shelf stations across the eastern coast of Antarctic Peninsula. Figure S2: Representative profiles of reactive pore water compounds at the five shelf stations [98]. Figure S3: Schematic illustration of the pore-water profiles that were typical for heavy ice cover (Shelf St1) (A) and low ice cover (Shelf St4) (B) of this study. Figure S4: Representative profiles of the depth distribution of putative Fe-reducing bacteria in relation to dissolved/pore-water iron (DFe) concentrations. Figure S5: Representative profiles of the depth distribution of putative Fe-reducing bacteria in relation to dissolved/pore-water iron (DFe) concentrations.

**Author Contributions:** Conceptualization, M.M., M.B. and M.H.; Fieldwork, M.B. and M.H.; molecular genetic analysis, M.B. and M.M.; geochemical analysis, M.B., M.H., S.H. and S.K.; data analysis, M.B. and M.M.; writing—original draft preparation, M.B. and M.M.; writing—review and editing, M.B., M.M., M.H., S.H. and S.K.; supervision, M.M. and M.H.; funding acquisition, M.H. All authors have read and agreed to the published version of the manuscript.

**Funding:** This study was funded by the AWI Grant-No. AWI_PS118_05, with open access funding enabled and organized by Project DEAL.

**Institutional Review Board Statement:** Not applicable.

**Data Availability Statement:** Sequence data for this study have been deposited in the European Nucleotide Archive (ENA) at EMBL-EBI under accession number PRJEB57442 (https://www.ebi.ac.uk/ena/data/view/PRJEB57442), using the data brokerage service of the German Federation for Biological Data GFBio, (accessed on 9 June 2023) [99].

**Acknowledgments:** The authors thank the captain and crew members of RV POLARSTERN during the PS118 expedition as well as Jakob Barz and Swantje Rogge (HGF-MPG Joint Research Group for Deep-Sea Ecology and Technology) for technical support. The authors are also grateful to Katja Metfies for support with Illumina sequencing.

**Conflicts of Interest:** The authors declare no conflict of interest. The funders had no role in the design of the study; in the collection, analyses, or interpretation of data; in the writing of the manuscript; or in the decision to publish the results.

## References

1. Elderfield, H. Element cycling in bottom sediments. *Philos. Trans. R. Soc. Lond.* **1985**, *315*, 19–23.
2. Shaw, T.J.; Gieskes, J.M.; Jahnke, R.A. Early diagenesis in differing depositional environments: The response of transition metals in pore water. *Geochim. Cosmochim. Acta* **1990**, *54*, 1233–1246. [CrossRef]
3. Monien, P.; Lettmann, K.A.; Monien, D.; Asendorf, S.; Wölfl, A.-C.; Lim, C.H.; Thal, J.; Schnetger, B.; Brumsack, H.-J. Redox conditions and trace metal cycling in coastal sediments from the maritime Antarctic. *Geochim. Cosmochim. Acta* **2014**, *141*, 26–44. [CrossRef]
4. Jørgensen, B.B.; Kasten, S. Sulfur cycling and methane oxidation. In *Marine Geochemistry*; Springer: Berlin/Heidelberg, Germany, 2006; pp. 271–309.
5. de Haas, H.; van Weering, T.C.; de Stigter, H. Organic carbon in shelf seas: Sinks or sources, processes and products. *Cont. Shelf Res.* **2002**, *22*, 691–717. [CrossRef]
6. Burdige, D.J. Preservation of Organic Matter in Marine Sediments: Controls, Mechanisms, and an Imbalance in Sediment Organic Carbon Budgets? *Chem. Rev.* **2007**, *107*, 467–485. [CrossRef]
7. Canfield, D.E. Organic matter oxidation in marine sediments. In *Interactions of C, N, P and S Biogeochemical Cycles and Global Change*; Springer: Berlin/Heidelberg, Germany, 1993; pp. 333–363.
8. Froelich, P.N.; Klinkhammer, G.; Bender, M.L.; Luedtke, N.; Heath, G.R.; Cullen, D.; Dauphin, P.; Hammond, D.; Hartman, B.; Maynard, V. Early oxidation of organic matter in pelagic sediments of the eastern equatorial Atlantic: Suboxic diagenesis. *Geochim. Cosmochim. Acta* **1979**, *43*, 1075–1090. [CrossRef]
9. Stumm, W.; Morgan, J.J. *Aquatic Chemistry: Chemical Equilibria and Rates in Natural Waters*; John Wiley & Sons: Hoboken, NJ, USA, 2012; Volume 126.
10. Canfield, D.E.; Thamdrup, B. Towards a consistent classification scheme for geochemical environments, or, why we wish the term 'suboxic' would go away. *Geobiology* **2009**, *7*, 385–392. [CrossRef]
11. Berner, R.A. *Early Diagenesis: A Theoretical Approach*; Princeton University Press: Princeton, NJ, USA, 1980.

12. D'Hondt, S.; Jørgensen, B.B.; Miller, D.J.; Batzke, A.; Blake, R.; Cragg, B.A.; Cypionka, H.; Dickens, G.R.; Ferdelman, T.; Hinrichs, K.-U. Distributions of microbial activities in deep subseafloor sediments. *Science* **2004**, *306*, 2216–2221. [CrossRef] [PubMed]
13. D'Hondt, S.; Rutherford, S.; Spivack, A.J. Metabolic activity of subsurface life in deep-sea sediments. *Science* **2002**, *295*, 2067–2070. [CrossRef] [PubMed]
14. Falkowski, P.G.; Fenchel, T.; Delong, E.F. The microbial engines that drive Earth's biogeochemical cycles. *Science* **2008**, *320*, 1034–1039. [CrossRef] [PubMed]
15. Azam, F.; Malfatti, F. Microbial structuring of marine ecosystems. *Nat. Rev. Microbiol.* **2007**, *5*, 782–791. [CrossRef] [PubMed]
16. Kasten, S.; Zabel, M.; Heuer, V.; Hensen, C. Processes and signals of nonsteady-state diagenesis in deep-sea sediments and their pore waters. In *The South Atlantic in the Late Quaternary*; Springer: Berlin/Heidelberg, Germany, 2003; pp. 431–459.
17. Canfield, D.E.; Thamdrup, B.; Hansen, J.W. The anaerobic degradation of organic matter in Danish coastal sediments: Iron reduction, manganese reduction, and sulfate reduction. *Geochim. Cosmochim. Acta* **1993**, *57*, 3867–3883. [CrossRef]
18. Zonneveld, K.A.; Versteegh, G.J.; Kasten, S.; Eglinton, T.I.; Emeis, K.-C.; Huguet, C.; Koch, B.P.; de Lange, G.J.; de Leeuw, J.W.; Middelburg, J.J. Selective preservation of organic matter in marine environments; processes and impact on the sedimentary record. *Biogeosciences* **2010**, *7*, 483–511. [CrossRef]
19. Ravenschlag, K.; Sahm, K.; Knoblauch, C.; Jørgensen, B.B.; Amann, R. Community structure, cellular rRNA content, and activity of sulfate-reducing bacteria in marine Arctic sediments. *Appl. Environ. Microbiol.* **2000**, *66*, 3592–3602. [CrossRef] [PubMed]
20. Jørgensen, S.L.; Hannisdal, B.; Lanzén, A.; Baumberger, T.; Flesland, K.; Fonseca, R.; Øvreås, L.; Steen, I.H.; Thorseth, I.H.; Pedersen, R.B. Correlating microbial community profiles with geochemical data in highly stratified sediments from the Arctic Mid-Ocean Ridge. *Proc. Natl. Acad. Sci. USA* **2012**, *109*, E2846–E2855. [CrossRef] [PubMed]
21. Sogin, M.L.; Morrison, H.G.; Huber, J.A.; Welch, D.M.; Huse, S.M.; Neal, P.R.; Arrieta, J.M.; Herndl, G.J. Microbial diversity in the deep sea and the underexplored "rare biosphere". *Proc. Natl. Acad. Sci. USA* **2006**, *103*, 12115–12120. [CrossRef]
22. Ruff, S.E.; Probandt, D.; Zinkann, A.-C.; Iversen, M.H.; Klaas, C.; Würzberg, L.; Krombholz, N.; Wolf-Gladrow, D.; Amann, R.; Knittel, K. Indications for algae-degrading benthic microbial communities in deep-sea sediments along the Antarctic Polar Front. *Deep. Sea Res. Part II Top. Stud. Oceanogr.* **2014**, *108*, 6–16. [CrossRef]
23. Bienhold, C.; Boetius, A.; Ramette, A. The energy–diversity relationship of complex bacterial communities in Arctic deep-sea sediments. *ISME J.* **2012**, *6*, 724–732. [CrossRef]
24. Molari, M.; Janssen, F.; Vonnahme, T.R.; Wenzhöfer, F.; Boetius, A. The contribution of microbial communities in polymetallic nodules to the diversity of the deep-sea microbiome of the Peru Basin (4130–4198 m depth). *Biogeosciences* **2020**, *17*, 3203–3222. [CrossRef]
25. Buongiorno, J.; Herbert, L.C.; Wehrmann, L.M.; Michaud, A.B.; Laufer, K.; Røy, H.; Jørgensen, B.B.; Szynkiewicz, A.; Faiia, A.; Yeager, K.M.; et al. Complex Microbial Communities Drive Iron and Sulfur Cycling in Arctic Fjord Sediments. *Appl. Environ. Microbiol.* **2019**, *85*, e00949-19. [CrossRef] [PubMed]
26. Wunder, L.C.; Aromokeye, D.A.; Yin, X.; Richter-Heitmann, T.; Willis-Poratti, G.; Schnakenberg, A.; Otersen, C.; Dohrmann, I.; Römer, M.; Bohrmann, G.; et al. Iron and sulfate reduction structure microbial communities in (sub-)Antarctic sediments. *ISME J.* **2021**, *15*, 3587–3604. [CrossRef] [PubMed]
27. Oni, O.; Miyatake, T.; Kasten, S.; Richter-Heitmann, T.; Fischer, D.; Wagenknecht, L.; Ksenofontov, V.; Kulkarni, A.; Blumers, M.; Shylin, S.; et al. Distinct microbial populations are tightly linked to the profile of dissolved iron in the methanic sediments of the Helgoland mud area, North Sea. *Front. Microbiol.* **2015**, *6*, 365. [CrossRef] [PubMed]
28. Schnakenberg, A.; Aromokeye, D.A.; Kulkarni, A.; Maier, L.; Wunder, L.C.; Richter-Heitmann, T.; Pape, T.; Ristova, P.P.; Bühring, S.I.; Dohrmann, I.; et al. Electron Acceptor Availability Shapes Anaerobically Methane Oxidizing Archaea (ANME) Communities in South Georgia Sediments. *Front. Microbiol.* **2021**, *12*, 617280. [CrossRef] [PubMed]
29. Savidge, G.; Harbour, D.; Gilpin, L.; Boyd, P. Phytoplankton distributions and production in the Bellingshausen Sea, Austral spring 1992. *Deep. Sea Res. Part II Top. Stud. Oceanogr.* **1995**, *42*, 1201–1224. [CrossRef]
30. Smith, C.R.; Mincks, S.; DeMaster, D.J. A synthesis of bentho-pelagic coupling on the Antarctic shelf: Food banks, ecosystem inertia and global climate change. *Deep. Sea Res. Part II Top. Stud. Oceanogr.* **2006**, *53*, 875–894. [CrossRef]
31. Smith, R.C.; Baker, K.S.; Dierssen, H.M.; Stammerjohn, S.E.; Vernet, M. Variability of primary production in an Antarctic marine ecosystem as estimated using a multi-scale sampling strategy. *Am. Zool.* **2001**, *41*, 40–56. [CrossRef]
32. Baloza, M.; Henkel, S.; Geibert, W.; Kasten, S.; Holtappels, M. Benthic Carbon Remineralization and Iron Cycling in Relation to Sea Ice Cover Along the Eastern Continental Shelf of the Antarctic Peninsula. *J. Geophys. Res. Ocean.* **2022**, *127*, e2021JC018401. [CrossRef]
33. Currie, A.A.; Marshall, A.J.; Lohrer, A.M.; Cummings, V.J.; Seabrook, S.; Cary, S.C. Sea Ice Dynamics Drive Benthic Microbial Communities in McMurdo Sound, Antarctica. *Front. Microbiol.* **2021**, *12*, 3189. [CrossRef]
34. Learman, D.R.; Henson, M.W.; Thrash, J.C.; Temperton, B.; Brannock, P.M.; Santos, S.R.; Mahon, A.R.; Halanych, K.M. Biogeochemical and Microbial Variation across 5500 km of Antarctic Surface Sediment Implicates Organic Matter as a Driver of Benthic Community Structure. *Front. Microbiol.* **2016**, *7*, 284. [CrossRef]
35. Abell, G.C.; Bowman, J.P. Ecological and biogeographic relationships of class Flavobacteria in the Southern Ocean. *FEMS Microbiol. Ecol.* **2005**, *51*, 265–277. [CrossRef]

36. Cho, H.; Hwang, C.Y.; Kim, J.-G.; Kang, S.; Knittel, K.; Choi, A.; Kim, S.-H.; Rhee, S.-K.; Yang, E.J.; Lee, S.; et al. A Unique Benthic Microbial Community Underlying the Phaeocystis antarctica-Dominated Amundsen Sea Polynya, Antarctica: A Proxy for Assessing the Impact of Global Changes. *Front. Mar. Sci.* **2020**, *6*, 797. [CrossRef]
37. Martin, J.H.; Gordon, R.M.; Fitzwater, S.E. Iron in Antarctic waters. *Nature* **1990**, *345*, 156–158. [CrossRef]
38. Boyd, P.W.; Jickells, T.; Law, C.; Blain, S.; Boyle, E.; Buesseler, K.; Coale, K.; Cullen, J.; De Baar, H.J.; Follows, M. Mesoscale iron enrichment experiments 1993–2005: Synthesis and future directions. *Science* **2007**, *315*, 612–617. [CrossRef]
39. Martin, J.H. Glacial-interglacial $CO_2$ change: The iron hypothesis. *Paleoceanography* **1990**, *5*, 1–13. [CrossRef]
40. Raiswell, R.; Benning, L.G.; Tranter, M.; Tulaczyk, S. Bioavailable iron in the Southern Ocean: The significance of the iceberg conveyor belt. *Geochem. Trans.* **2008**, *9*, 7. [CrossRef]
41. Raiswell, R.; Hawkings, J.R.; Benning, L.G.; Baker, A.R.; Death, R.; Albani, S.; Mahowald, N.; Krom, M.D.; Poulton, S.W.; Wadham, J.; et al. Potentially bioavailable iron delivery by iceberg-hosted sediments and atmospheric dust to the polar oceans. *Biogeosciences* **2016**, *13*, 3887–3900. [CrossRef]
42. Lancelot, C.; de Montety, A.; Goosse, H.; Becquevort, S.; Schoemann, V.; Pasquer, B.; Vancoppenolle, M. Spatial distribution of the iron supply to phytoplankton in the Southern Ocean: A model study. *Biogeosciences* **2009**, *6*, 2861–2878. [CrossRef]
43. Wadham, J.L.; De'ath, R.; Monteiro, F.M.; Tranter, M.; Ridgwell, A.; Raiswell, R.; Tulaczyk, S. The potential role of the Antarctic Ice Sheet in global biogeochemical cycles. *Earth Environ. Sci. Trans. R. Soc. Edinb.* **2013**, *104*, 55–67. [CrossRef]
44. Measures, C.; Brown, M.; Selph, K.; Apprill, A.; Zhou, M.; Hatta, M.; Hiscock, W. The influence of shelf processes in delivering dissolved iron to the HNLC waters of the Drake Passage, Antarctica. *Deep. Sea Res. Part II Top. Stud. Oceanogr.* **2013**, *90*, 77–88. [CrossRef]
45. Henkel, S.; Kasten, S.; Hartmann, J.F.; Silva-Busso, A.; Staubwasser, M. Iron cycling and stable Fe isotope fractionation in Antarctic shelf sediments, King George Island. *Geochim. Cosmochim. Acta* **2018**, *237*, 320–338. [CrossRef]
46. Nielsdóttir, M.C.; Bibby, T.S.; Moore, C.M.; Hinz, D.J.; Sanders, R.; Whitehouse, M.; Korb, R.; Achterberg, E.P. Seasonal and spatial dynamics of iron availability in the Scotia Sea. *Mar. Chem.* **2012**, *130–131*, 62–72. [CrossRef]
47. Hatta, M.; Measures, C.; Selph, K.; Zhou, M.; Hiscock, W. Iron fluxes from the shelf regions near the South Shetland Islands in the Drake Passage during the austral-winter 2006. *Deep. Sea Res. Part II Top. Stud. Oceanogr.* **2013**, *90*, 89–101. [CrossRef]
48. Borrione, I.; Aumont, O.; Nielsdóttir, M.; Schlitzer, R. Sedimentary and atmospheric sources of iron around South Georgia, Southern Ocean: A modelling perspective. *Biogeosciences* **2014**, *11*, 1981–2001. [CrossRef]
49. Aromokeye, D.A.; Willis-Poratti, G.; Wunder, L.C.; Yin, X.; Wendt, J.; Richter-Heitmann, T.; Henkel, S.; Vázquez, S.; Elvert, M.; Mac Cormack, W. Macroalgae degradation promotes microbial iron reduction via electron shuttling in coastal Antarctic sediments. *Environ. Int.* **2021**, *156*, 106602. [CrossRef] [PubMed]
50. Thamdrup, B.; Rosselló-Mora, R.; Amann, R. Microbial manganese and sulfate reduction in Black Sea shelf sediments. *Appl. Environ. Microbiol.* **2000**, *66*, 2888–2897. [CrossRef] [PubMed]
51. Henkel, S.; Kasten, S.; Poulton, S.W.; Staubwasser, M. Determination of the stable iron isotopic composition of sequentially leached iron phases in marine sediments. *Chem. Geol.* **2016**, *421*, 93–102. [CrossRef]
52. Vandieken, V.; Thamdrup, B. Identification of acetate-oxidizing bacteria in a coastal marine surface sediment by RNA-stable isotope probing in anoxic slurries and intact cores. *FEMS Microbiol. Ecol.* **2013**, *84*, 373–386. [CrossRef]
53. Vandieken, V.; Mußmann, M.; Niemann, H.; Jørgensen, B.B. Desulfuromonas svalbardensis sp. nov. and Desulfuromusa ferrireducens sp. nov., psychrophilic, Fe (III)-reducing bacteria isolated from Arctic sediments, Svalbard. *Int. J. Syst. Evol. Microbiol.* **2006**, *56*, 1133–1139. [CrossRef]
54. Vandieken, V.; Finke, N.; Jørgensen, B.B. Pathways of carbon oxidation in an Arctic fjord sediment (Svalbard) and isolation of psychrophilic and psychrotolerant Fe (III)-reducing bacteria. *Mar. Ecol. Prog. Ser.* **2006**, *322*, 29–41. [CrossRef]
55. Holmes, D.E.; Nicoll, J.S.; Bond, D.R.; Lovley, D.R. Potential role of a novel psychrotolerant member of the family Geobacteraceae, Geopsychrobacter electrodiphilus gen. nov., sp. nov., in electricity production by a marine sediment fuel cell. *Appl. Environ. Microbiol.* **2004**, *70*, 6023–6030. [CrossRef]
56. Aromokeye, D.A.; Richter-Heitmann, T.; Oni, O.E.; Kulkarni, A.; Yin, X.; Kasten, S.; Friedrich, M.W. Temperature controls crystalline iron oxide utilization by microbial communities in methanic ferruginous marine sediment incubations. *Front. Microbiol.* **2018**, *9*, 2574. [CrossRef] [PubMed]
57. Kashefi, K.; Holmes, D.E.; Baross, J.A.; Lovley, D.R. Thermophily in the Geobacteraceae: *Geothermobacter ehrlichii* gen. nov., sp. nov., a novel thermophilic member of the Geobacteraceae from the "Bag City" hydrothermal vent. *Appl. Environ. Microbiol.* **2003**, *69*, 2985–2993. [CrossRef]
58. Ravenschlag, K.; Sahm, K.; Pernthaler, J.; Amann, R. High bacterial diversity in permanently cold marine sediments. *Appl. Environ. Microbiol.* **1999**, *65*, 3982–3989. [CrossRef]
59. Fetterer, F.; Knowles, K.; Meier, W.N.; Savoie, M.; Windnagel, A.K. *Sea Ice Index, Version 3. [Years 1978–2019]*; NSIDC: National Snow and Ice Data Center: Boulder, CO, USA, 2017. [CrossRef]
60. Spreen, G.; Kaleschke, L.; Heygster, G. Sea ice remote sensing using AMSR-E 89-GHz channels. *J. Geophys. Res. Ocean.* **2008**, *113*, 148–227. [CrossRef]
61. Martin, M. Cutadapt removes adapter sequences from high-throughput sequencing reads. *EMBnet J.* **2011**, *17*, 10–12. [CrossRef]
62. Callahan, B.J.; McMurdie, P.J.; Rosen, M.J.; Han, A.W.; Johnson, A.J.A.; Holmes, S.P. DADA2: High-resolution sample inference from Illumina amplicon data. *Nat. Methods* **2016**, *13*, 581–583. [CrossRef]

63. Quast, C.; Pruesse, E.; Yilmaz, P.; Gerken, J.; Schweer, T.; Yarza, P.; Peplies, J.; Glöckner, F.O. The SILVA ribosomal RNA gene database project: Improved data processing and web-based tools. *Nucleic Acids Res.* **2012**, *41*, D590–D596. [CrossRef] [PubMed]
64. Gobet, A.; Boetius, A.; Ramette, A. Ecological coherence of diversity patterns derived from classical fingerprinting and N ext G eneration S equencing techniques. *Environ. Microbiol.* **2014**, *16*, 2672–2681. [CrossRef]
65. Team, R.C. *R: A Language and Environment for Statistical Computing*; R Foundation for Statistical Computing: Vienna, Austria. Available online: https://www.R-project.org/ (accessed on 12 June 2022).
66. McMurdie, P.J.; Holmes, S. phyloseq: An R package for reproducible interactive analysis and graphics of microbiome census data. *PLoS ONE* **2013**, *8*, e61217. [CrossRef]
67. Oksanen, J.; Blanchet, F.G.; Kindt, R.; Legendre, P.; Minchin, P.; O'hara, R.; Simpson, G.; Solymos, P.; Stevens, M.H.H.; Wagner, H. Community ecology package. *R Package Version* **2013**, *2*, 321–326.
68. Van den Boogaart, K.G.; Tolosana-Delgado, R. *Analyzing Compositional Data with R*; Springer: Berlin/Heidelberg, Germany, 2013; Volume 122.
69. Fernandes, A.; Macklaim, J.; Linn, T.; Reid, G.; Gloor, G. ANOVA-like differential gene expression analysis of single-organism and meta-RNA-seq. *PLoS ONE* **2013**, *8*, e67019. [CrossRef] [PubMed]
70. Park, S.-J.; Park, B.-J.; Jung, M.-Y.; Kim, S.-J.; Chae, J.-C.; Roh, Y.; Forwick, M.; Yoon, H.-I.; Rhee, S.-K. Influence of Deglaciation on Microbial Communities in Marine Sediments Off the Coast of Svalbard, Arctic Circle. *Microb. Ecol.* **2011**, *62*, 537–548. [CrossRef] [PubMed]
71. Li, H.; Yu, Y.; Luo, W.; Zeng, Y.; Chen, B. Bacterial diversity in surface sediments from the Pacific Arctic Ocean. *Extremophiles* **2009**, *13*, 233–246. [CrossRef]
72. Hubert, C.; Loy, A.; Nickel, M.; Arnosti, C.; Baranyi, C.; Brüchert, V.; Ferdelman, T.; Finster, K.; Christensen, F.M.; Rosa de Rezende, J. A constant flux of diverse thermophilic bacteria into the cold Arctic seabed. *Science* **2009**, *325*, 1541–1544. [CrossRef]
73. Bowman, J.P.; McCammon, S.A.; Gibson, J.A.E.; Robertson, L.; Nichols, P.D. Prokaryotic Metabolic Activity and Community Structure in Antarctic Continental Shelf Sediments. *Appl. Environ. Microbiol.* **2003**, *69*, 2448–2462. [CrossRef]
74. Purdy, K.J.; Nedwell, D.B.; Embley, T.M. Analysis of the sulfate-reducing bacterial and methanogenic archaeal populations in contrasting Antarctic sediments. *Appl. Environ. Microbiol.* **2003**, *69*, 3181–3191. [CrossRef]
75. Teske, A.; Durbin, A.; Ziervogel, K.; Cox, C.; Arnosti, C. Microbial Community Composition and Function in Permanently Cold Seawater and Sediments from an Arctic Fjord of Svalbard. *Appl. Environ. Microbiol.* **2011**, *77*, 2008–2018. [CrossRef]
76. Cardman, Z.; Arnosti, C.; Durbin, A.; Ziervogel, K.; Cox, C.; Steen, A.D.; Teske, A. Verrucomicrobia are candidates for polysaccharide-degrading bacterioplankton in an arctic fjord of Svalbard. *Appl. Environ. Microbiol.* **2014**, *80*, 3749–3756. [CrossRef] [PubMed]
77. Ruff, S.E.; Arnds, J.; Knittel, K.; Amann, R.; Wegener, G.; Ramette, A.; Boetius, A. Microbial communities of deep-sea methane seeps at Hikurangi continental margin (New Zealand). *PLoS ONE* **2013**, *8*, e72627. [CrossRef]
78. Nunoura, T.; Oida, H.; Nakaseama, M.; Kosaka, A.; Ohkubo, S.B.; Kikuchi, T.; Kazama, H.; Hosoi-Tanabe, S.; Nakamura, K.; Kinoshita, M.; et al. Archaeal diversity and distribution along thermal and geochemical gradients in hydrothermal sediments at the Yonaguni Knoll IV hydrothermal field in the Southern Okinawa trough. *Appl. Environ. Microbiol.* **2010**, *76*, 1198–1211. [CrossRef]
79. Pischedda, L.; Militon, C.; Gilbert, F.; Cuny, P. Characterization of specificity of bacterial community structure within the burrow environment of the marine polychaete Hediste (Nereis) diversicolor. *Res. Microbiol.* **2011**, *162*, 1033–1042. [CrossRef] [PubMed]
80. Beal, E.J.; House, C.H.; Orphan, V.J. Manganese- and iron-dependent marine methane oxidation. *Science* **2009**, *325*, 184–187. [CrossRef] [PubMed]
81. Lösekann, T.; Knittel, K.; Nadalig, T.; Fuchs, B.; Niemann, H.; Boetius, A.; Amann, R. Diversity and abundance of aerobic and anaerobic methane oxidizers at the Haakon Mosby Mud Volcano, Barents Sea. *Appl. Environ. Microbiol.* **2007**, *73*, 3348–3362. [CrossRef] [PubMed]
82. Vaughan, D.G.; Marshall, G.J.; Connolley, W.M.; Parkinson, C.; Mulvaney, R.; Hodgson, D.A.; King, J.C.; Pudsey, C.J.; Turner, J. Recent Rapid Regional Climate Warming on the Antarctic Peninsula. *Clim. Change* **2003**, *60*, 243–274. [CrossRef]
83. Eayrs, C.; Li, X.; Raphael, M.N.; Holland, D.M. Rapid decline in Antarctic sea ice in recent years hints at future change. *Nat. Geosci.* **2021**, *14*, 460–464. [CrossRef]
84. Mitchell, B.G.; Holm-Hansen, O. Observations of modeling of the Antartic phytoplankton crop in relation to mixing depth. *Deep. Sea Res. Part A Oceanogr. Res. Pap.* **1991**, *38*, 981–1007. [CrossRef]
85. Sakshaug, E.; Slagstad, D.; Holm-Hansen, O. Factors controlling the development of phytoplankton blooms in the Antarctic Ocean—A mathematical model. *Mar. Chem.* **1991**, *35*, 259–271. [CrossRef]
86. Schloss, I.R.; Ferreyra, G.A.; Ruiz-Pino, D. Phytoplankton biomass in Antarctic shelf zones: A conceptual model based on Potter Cove, King George Island. *J. Mar. Syst.* **2002**, *36*, 129–143. [CrossRef]
87. Garibotti, I.A.; Vernet, M.; Smith, R.C.; Ferrario, M.E. Interannual variability in the distribution of the phytoplankton standing stock across the seasonal sea-ice zone west of the Antarctic Peninsula. *J. Plankton Res.* **2005**, *27*, 825–843. [CrossRef]
88. Teeling, H.; Fuchs, B.M.; Becher, D.; Klockow, C.; Gardebrecht, A.; Bennke, C.M.; Kassabgy, M.; Huang, S.; Mann, A.J.; Waldmann, J. Substrate-controlled succession of marine bacterioplankton populations induced by a phytoplankton bloom. *Science* **2012**, *336*, 608–611. [CrossRef]

89. Bano, N.; Hollibaugh, J.T. Phylogenetic Composition of Bacterioplankton Assemblages from the Arctic Ocean. *Appl. Environ. Microbiol.* **2002**, *68*, 505–518. [CrossRef]
90. Roden, E.E.; Lovley, D.R. Dissimilatory Fe (III) reduction by the marine microorganism Desulfuromonas acetoxidans. *Appl. Environ. Microbiol.* **1993**, *59*, 734–742. [CrossRef]
91. Jørgensen, B.B.; Laufer, K.; Michaud, A.B.; Wehrmann, L.M. Biogeochemistry and microbiology of high Arctic marine sediment ecosystems—Case study of Svalbard fjords. *Limnol. Oceanogr.* **2021**, *66*, S273–S292. [CrossRef]
92. Canfield, D.E. Reactive iron in marine sediments. *Geochim. Cosmochim. Acta* **1989**, *53*, 619–632. [CrossRef]
93. Riedinger, N.; Brunner, B.; Krastel, S.; Arnold, G.L.; Wehrmann, L.M.; Formolo, M.J.; Beck, A.; Bates, S.M.; Henkel, S.; Kasten, S. Sulfur cycling in an iron oxide-dominated, dynamic marine depositional system: The Argentine continental margin. *Front. Earth Sci.* **2017**, *5*, 33. [CrossRef]
94. Wehrmann, L.M.; Riedinger, N.; Brunner, B.; Kamyshny, A.; Hubert, C.R.J.; Herbert, L.C.; Brüchert, V.; Jørgensen, B.B.; Ferdelman, T.G.; Formolo, M.J. Iron-controlled oxidative sulfur cycling recorded in the distribution and isotopic composition of sulfur species in glacially influenced fjord sediments of west Svalbard. *Chem. Geol.* **2017**, *466*, 678–695. [CrossRef]
95. Michaud, A.B.; Laufer, K.; Findlay, A.; Pellerin, A.; Antler, G.; Turchyn, A.V.; Røy, H.; Wehrmann, L.M.; Jørgensen, B.B. Glacial influence on the iron and sulfur cycles in Arctic fjord sediments (Svalbard). *Geochim. Cosmochim. Acta* **2020**, *280*, 423–440. [CrossRef]
96. Santelli, C.M.; Orcutt, B.N.; Banning, E.; Bach, W.; Moyer, C.L.; Sogin, M.L.; Staudigel, H.; Edwards, K.J. Abundance and diversity of microbial life in ocean crust. *Nature* **2008**, *453*, 653–656. [CrossRef] [PubMed]
97. Taylor, K.E.; Stouffer, R.J.; Meehl, G.A. An overview of CMIP5 and the experiment design. *Bull. Am. Meteorol. Soc.* **2012**, *93*, 485–498. [CrossRef]
98. Weston, N.B.; Porubsky, W.P.; Samarkin, V.A.; Erickson, M.; Macavoy, S.E.; Joye, S.B. Porewater stoichiometry of terminal metabolic products, sulfate, and dissolved organic carbon and nitrogen in estuarine intertidal creek-bank sediments. *Biogeochemistry* **2006**, *77*, 375–408.
99. Diepenbroek, M.; Glöckner, F.O.; Grobe, P.; Güntsch, A.; Huber, R.; König-Ries, B.; Kostadinov, I.; Nieschulze, J.; Seeger, B.; Tolksdorf, R. Towards an integrated biodiversity and ecological research data management and archiving platform: The German federation for the curation of biological data (GFBio). In *GI-Jahrestagung*; German Informatics Society: Bonn, Germany, 2014.